Metastatic cells exploit their stoichiometric niche in the network of cancer ecosystems

Simon P Castillo, Rolando A Rebolledo, Matías Arim, Michael E Hochberg, Pablo A Marquet

CANCER

Metastatic cells exploit their stoichiometric niche in the network of cancer ecosystems

Simon P. Castillo[1]*†, Rolando A. Rebolledo[2,3], Matías Arim[4], Michael E. Hochberg[5,6], Pablo A. Marquet[1,6,7,8]*

Metastasis is a nonrandom process with varying degrees of organotropism—specific source-acceptor seeding. Understanding how patterns between source and acceptor tumors emerge remains a challenge in oncology. We hypothesize that organotropism results from the macronutrient niche of cells in source and acceptor organs. To test this, we constructed and analyzed a metastatic network based on 9303 records across 28 tissue types. We found that the topology of the network is nested and modular with scale-free degree distributions, reflecting organotropism along a specificity/generality continuum. The variation in topology is significantly explained by the matching of metastatic cells to their stoichiometric niche. Specifically, successful metastases are associated with higher phosphorus content in the acceptor compared to the source organ, due to metabolic constraints in proliferation crucial to the invasion of new tissues. We conclude that metastases are codetermined by processes at source and acceptor organs, where phosphorus content is a limiting factor orchestrating tumor ecology.

INTRODUCTION

Migration and successful colonization of a novel organ by tumor cells from a primary tumor is the leading cause of mortality in patients with solid tumors (*1*), representing one of the main challenges for treating many types of cancer (*2*). Puzzling characteristics of metastasis include organ-to-organ variation in susceptibility to metastasis, and primary tumors can metastasize to different or sometimes to specific organs—a phenomenon known as organotropism (*3*). To explain metastatic diversity, Paget (*4*) proposed the "seed-and-soil" hypothesis: Metastasis requires adequate microenvironmental conditions in the acceptor organ or tissue (*5*). This explanation is analogous to the Grinnellian niche in ecology, whereby the persistence of a species in a given habitat is a function of the prevailing environmental conditions, which determine fitness (*6*). After Paget, Ewing (*7*) suggested that metastatic spread is explained by structural factors related to the vascular system and the proximity between source and acceptor sites. Ewing's hypothesis predicts that the probability of metastasis to a given organ depends on the number of arriving cancer cells (propagule pressure), which depends, in turn, on the development of primary tumors (*8*, *9*), the pool of circulating tumor cells (*10*), and blood flow (*11*–*14*) (i.e., connectivity). Despite research over the intervening decades, it is still unclear how general Paget's and Ewing's hypotheses are to explain observed metastatic patterns (*15*) and how they match with the observed molecular mechanisms, e.g., metabolic reprogramming (*16*), associated with metastasis (*17*, *18*).

Colonizing new tissues requires sufficient microenvironmental nutrients and energy throughout the cell cycle, which, in turn, requires adenosine 5′-triphosphate (ATP), ribonucleic acids (RNA) and ribosomal biogenesis, proteins, and overall, phosphorus (P). The growth rate hypothesis (*19*) predicts substantial P requirements for a growing tumor and success in metastasis (*20*). Metastasis would be mediated by the transport and utilization of phosphorus, for instance, for posttranscriptional protein modification, the generation of P-rich ribosomal RNA, and ribosomal proteins (*21*, *22*) to meet the demands of protein synthesis required during proliferation, as it has been shown in metastatic breast cancer (*23*). At a molecular level, the landscape of ribosomal protein transcripts differs across tissues (*24*), presenting opportunities to better understand how phosphorus could mediate cell proliferation, metastatic success, and organotropism.

In metabolic terms, the higher P metabolism of cancer cells is associated with a shift from a high ATP yield oxidative phosphorylation to aerobic glycolysis with a higher rate of ATP production but a lower energetic yield (Warburg effect) (*25*, *26*). The P-mediated enhancement of cell proliferation resulting from faster ATP production would present competitive advantages for metastatic propagules, allowing them to evade competitive exclusion from resident cells with higher ATP yield (*26*) and successfully metastasize (*27*). Cell proliferation is enhanced by redirecting P molecules to the synthesis of phosphatases and the overexpression of enzymes such as the reduced form of nicotinamide adenine dinucleotide phosphate oxidase (encoded by the *NOX* gene family), increasing the number of transporters and promoting angiogenesis (*20*, *28*). As the primary tumor grows, access to resources by tumor cells becomes increasingly nonuniform, exacerbating chemical gradients and competition between cells and potentially leading to dispersal (*20*, *29*). We hypothesize that competitive stresses lead to both a dispersive phenotype and the up-regulation of P metabolism for proliferation in the otherwise unfamiliar habitat at the acceptor organ site (*30*).

[1]Departamento de Ecología, Facultad de Ciencias Biológicas, Pontificia Universidad Católica de Chile, C.P. 8331150, Santiago, Chile. [2]Instituto de Ingeniería Biológica y Médica (IIBM), Pontificia Universidad Católica de Chile, Santiago, Chile. [3]Hepato-Pancreato-Biliary Surgery Unit, Surgery Service, Complejo Asistencial Dr. Sótero Del Río, Santiago, Chile. [4]Departamento de Ecologia y Gestion Ambiental, Centro Universitario Regional Este (CURE), Universidad de la República, Maldonado, Uruguay. [5]ISEM, University of Montpellier, Montpellier, France. [6]Santa Fe Institute, Santa Fe, NM 87501, USA. [7]Centro de Modelamiento Matemático, Universidad de Chile, International Research Laboratory 2807, CNRS, C.P. 8370456, Santiago, Chile. [8]Instituto de Sistemas Complejos de Valparaíso (ISCV), Valparaíso, Chile.
*Corresponding author. Email: spcastillo@mdanderson.org (S.P.C.); pmarquet@bio.puc.cl (P.A.M.)
†Present address: Department of Translational Molecular Pathology, Division of Pathology and Laboratory Medicine and Institute for Data Science in Oncology (IDSO), The University of Texas MD Anderson Cancer Center, Houston, TX 77030, USA.

Furthermore, we ponder that in the source tissue, the metabolic change associated with the neoplastic phenotype (glycolytic shift) endows the cancer cells with the ability to invade their home tissue (*26*, *31*). The up-regulated P metabolism of cancer cells constrains metastatic proliferation, which would only be successful in tissues where the P content is higher than the one associated with the primary tumor. High P tissues are where the metastatic phenotype will still have an advantage in enhancing the metastatic cell's fitness. Structural factors of the vascular system affect the incidence of metastases (*11*–*14*) since they affect the connectivity among organs and the intensity of the flow of metastatic propagules. Thus, topological connectivity and the varying levels of nutrients across organs (*30*) create a gradient in habitat suitability jointly determining the metastatic specificity between donor and acceptor tissues. We reason that the flow and selection of cancer cells in the metastatic network of source and acceptor organs will produce emergent patterns of organotropism based on stoichiometric niche opportunities (*32*).

RESULTS

The network structure of metastases

We study large-scale patterns in metastases across 28 organs based on 9303 published metastatic records (Fig. 1, A and B, and the Supplementary Materials), which allow us to quantify organotropism and reveal variation in the degree of generality and specificity in both primary tumors and metastatic sites. The topological measures of nestedness of the metastatic network quantify the variability in organotropism [temperature, 6.46; nestedness based on the overlap and decreasing fill (NODF2), 47.4; and weighted-interaction nestedness estimator (WINE), 0.84; Fig. 1C], which is significantly greater than the null models (fig. S1). Analogous to habitat patches (*33*), nestedness can arise as a macroscopic property (*34*) when there is a gradient in suitability leading to differences in colonization or extinction probabilities (*35*). In addition, a truncated power-law degree distribution, especially in the source organ degree distribution (Fig. 1D and table S1), indicates a large heterogeneity in organ connectivity, where some organs are highly connected to others through metastases, as is characteristic of ecological networks (*36*), although it should be interpreted carefully, considering the small size of the metastatic network. The network also shows significant modularity, evidencing densely connected groups of organs (z-score > 55, Fig. 1E and fig. S1). These modules were observed when primary tumors occur in organs with high cellular turnover (e.g., skin, stomach, small intestine, and lung), forming clusters with acceptor organs having lower cellular turnover but among the most metabolically active, such as the brain, thyroids, or adrenal glands (*37*). This pattern indicates potential drivers associated with cell proliferation, competition, and resource exploitation (*29*).

Moreover, to study the role of the vascular system in defining spatial relationships between organs in the sense of Ewing's structural hypothesis, we assembled a binary vascular matrix representing spatial relationships between organs as a function of shared main blood vessels. We tested the statistical association between the vascular matrix and the metastatic incidence matrix (Kendall's rank correlation). The correlation between the matrices of metastatic incidence and vascularity for 19 source/acceptor organs with defined local vascular topology is significant but small in magnitude (Kendall's rank correlation, tau = 0.126, z = 2.7, P = 0.007). These network patterns provide evidence of a connection between physiological and metastatic attributes.

Macronutrient heterogeneity, primary tumors, and successful metastases

Successful colonization emerges from the compatibility of the metastatic cell's niche and the acceptor's microenvironmental conditions (*38*). To test the P-driven metastatic colonization hypothesis, we reason that a higher likelihood of colonization would be possible in organs with resources to support higher energy production based on the metastatic cell's requirements needed to fulfil the demands of a fast proliferative strategy (*17*, *18*, *39*, *40*). The P content is a measure of phosphate-rich molecules, such as high-energy molecules (ATP), membrane phospholipids, signaling pathways, and RNA/DNA phosphodiester backbones (*21*, *22*), and it could give clues about an organ's conditions to support a demanding metabolism. Assuming metabolic constraints, phosphorus content is predicted to be correlated with the incidence of primary tumors and with metastatic potential. Specifically, in organs with low habitat quality (low tissue P content), cancer cells forming a primary tumor have stronger advantages due to their metabolic shift; hence, a negative association between age-adjusted cancer incidence rates and organ P content is expected, in a general sense, regardless of the organ being source or acceptor of metastases. In addition, a negative relationship between tissue P content and its number of links as a source (source degree, $\boldsymbol{k_S}$), a positive association with acceptor degree ($\boldsymbol{k_A}$), and the P difference (source-acceptor, $\boldsymbol{\Delta P}$) negatively correlated with the metastatic relative occurrences (number of occurrences for a source-acceptor pair over the total number of records). To assess the habitat quality of organs, we use literature estimates of phosphorus (P) content per gram of organ/tissues (*41*) for the source and acceptor organs. This information was available for 19 organs, involving 4934 metastatic records in the present database. The age-adjusted cancer incidence rates in primary tumors [from (*42*)] have a significant negative correlation with the organ's P content (N = 11, Pearson's $\rho = -0.78$, 95% confidence interval: −0.941 to −0.346, P = 0.0044; fig. S2). Regarding the metastatic cases, we found that primary tumors in low-P organs are more invasive in terms of the number of acceptor organs they reach, and this is manifested in a significant negative effect of P on $\boldsymbol{k_S}$ [negative binomial regression, effect estimate (1,16) = −593.99, $z = -2.72$, P = 0.007], while no significant effect of P content on $\boldsymbol{k_A}$ was detected [negative binomial regression, effect estimate (1,16) = 95.03, z = 0.74, P = 0.46]. The larger the phosphorus content in acceptor tissues in comparison to the source (negative $\boldsymbol{\Delta P}$), the higher the relative occurrence of metastasis [zero-inflated regression, R^2 = 0.96, occurrences (Poisson): effect estimate of $\boldsymbol{\Delta P} = -0.42$, SE = 0.013, $z = -32.13$, $P < 0.001$; absences (binomial): effect estimate of $\boldsymbol{\Delta P}$ = 0.61, SE = 0.103, z = 5.96, $P = 2.47 \times 10^{-9}$] (Fig. 2). Together, these results indicate that P limits both primary tumor incidence and metastatic spread. In particular, supporting the P hypothesis, a low P in the source relative to an acceptor organ may be necessary to generate metastases.

Phosphorus diversity across organs and structural properties of the metastatic network

Last, we sought to test whether the observed phosphorus variability across organs (Fig. 2) could contribute to explaining the

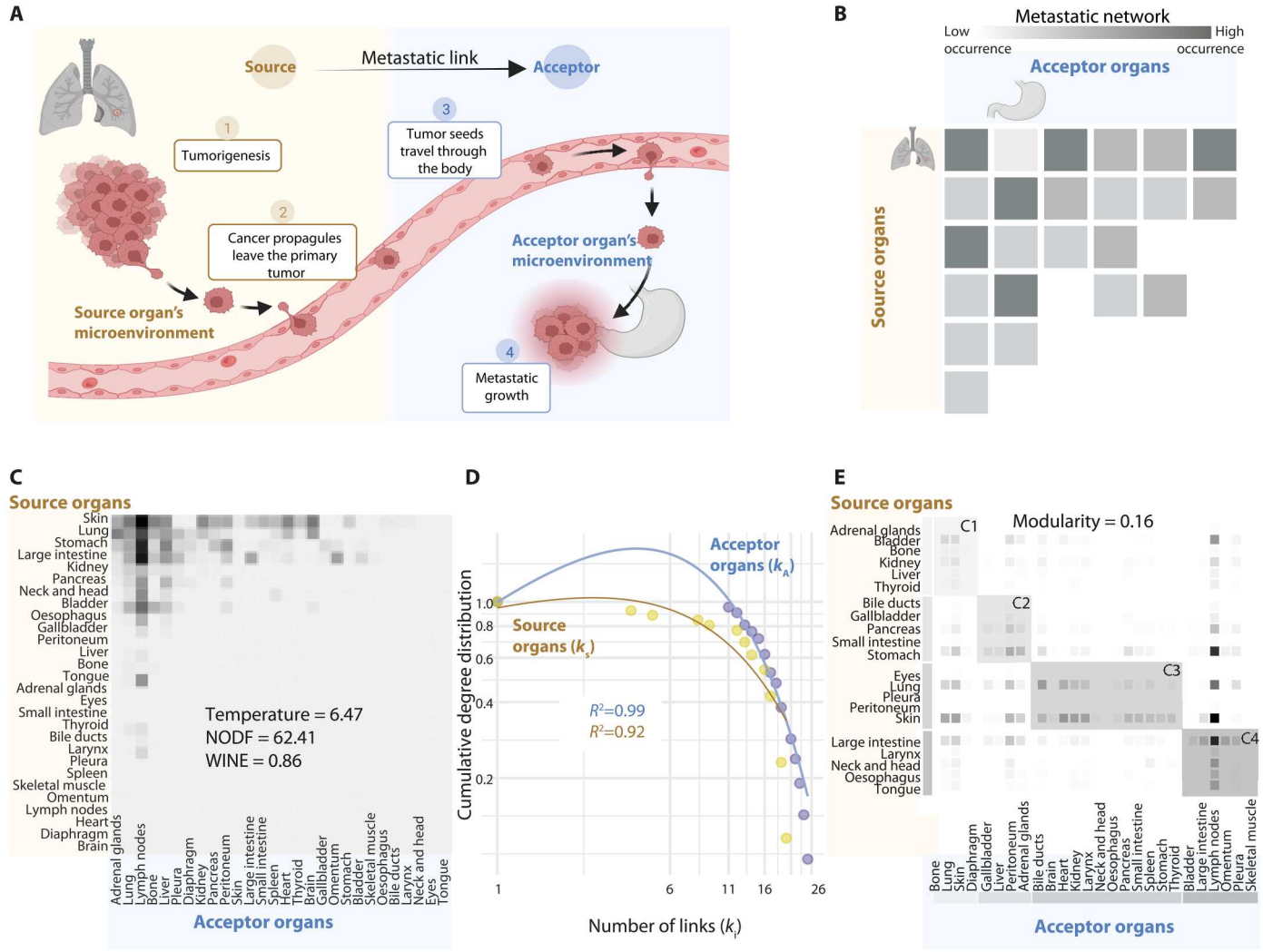

Fig. 1. The metastatic network. (**A**) The process of metastasis starts with tumorigenesis in a source organ and may continue with metastatic growth in a distant acceptor organ. A metastatic network recapitulates this complexity across source and acceptor organs. (**B**) Each entry in this illustrative metastatic network represents the number of occurrences of successful metastases from a source to an acceptor organ. We observed that the metastatic network (N = 28 organs, 9303 records of metastases) is nested (**C**), has a strongly asymmetric degree distribution (**D**) (lines represent a truncated power-law fit on the probability density function for $\boldsymbol{k_S}$ and $\boldsymbol{k_A}$), and is modular (**E**). (A) and (B) were made using BioRender (www.biorender.com).

macroscopic patterns observed in the metastasis network (Fig. 1). We simulated six scenarios of metastases in which the probability of metastasis depends on a subset of the observed organ's attributes: stem cell divisions of the source organ, blood flow through the organ, topological-vascular constraints producing propagules filtering in the liver in the case of gastrointestinal (GI) tumors, filter flow analysis sensu (*13*, *14*), and the source-acceptor difference in P ($\boldsymbol{\Delta P}$) (Fig. 3A). We include stem cell divisions (cumulative stem cell divisions per lifetime) as a driver of the probability of having a primary tumor in a particular organ (*43*) because it is a necessary condition for a metastatic occurrence. All the other variables are linked to the acceptor organ. Consistently, including $\boldsymbol{\Delta P}$ in the simulation produces a significantly higher correlation between observed and simulated metastatic relative occurrences (Fig. 3B). In addition, the simulation scenarios with $\boldsymbol{\Delta P}$ as a codeterminant of metastasis generate nested and modular metastatic networks similar to the observed values (Fig. 3C, figs. S3 and S4, and table S4). This suggests that the observed phosphorus difference as a proxy of habitat quality across organs contributes to generating observed macroscopic patterns of the network, along with the combined effect of stem cell divisions or propagule pressure mediated by blood flow.

DISCUSSION

Ecological constraints and the stoichiometric niche of metastatic cancer cells

Analogies from ecology (*44*, *45*) can bring new perspectives to understanding metastasis. Hence, the seed and soil hypothesis has guided our conceptual understanding of metastasis (*5*, *46*) but at the cost of focusing on single source-acceptor links and overemphasizing the attributes of the acceptor "soil" organ relative to the

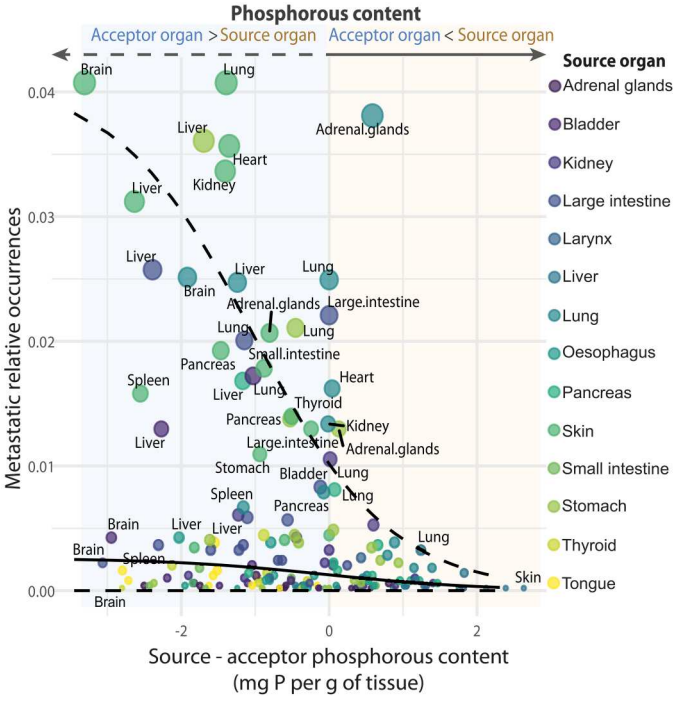

Fig. 2. The phosphorus niche of metastatic cells. Metastases tend to be successful when neoplastic cells migrate to an organ where P content is higher than in the source organ (excluding from/to bone metastases; see Materials and Methods). Metastatic relative occurrences are estimated for the 19 organs for which P content information was available (4934 cases). Point labels are the acceptor organ and the circle size metastatic relative occurrences. Lines are nonlinear quantile regressions for the first (bottom dashed line), fifth (solid line), and ninth (top dashed line) deciles. See an interactive plot at https://simonpcastillo.github.io/metastaticdiaspora.

source organ. By integrating the structural, seed-and-soil, and growth rate hypotheses powered by a network perspective, we provide a more general statistical assessment emphasizing the vital role played by tissue stoichiometry (*20*) in priming metastatic propagules and defining suitable conditions for metastasis. These microscopic molecular and cellular phenomena produce observed macroscopic patterns of metastasis.

Analogous to findings on the influence of nutrients in species invasions (*47*), our results indicate that phosphorus content is decisive for metastatic progression. The difference in phosphorus content between source and acceptor organs may act as an environmental filter, with metastatic propagules being more successful in habitats/organs with higher P content (*16*). Tumor cells from low-P organs will have better chances of survival and proliferation in acceptor tissues due to their low basal P requirements, having substantial competitive advantages in P-rich organs due to their faster phosphorus metabolism (*29*, *48*, *49*). Cancer onset may emerge by chance (*9*), but the stoichiometric landscape could configure tumor progression from the primary site and potential metastatic cascades and the habitat suitability present in the acceptor tissue such as nutrients or amino acids (*30*), where metabolic flexibility and plasticity are associated with the premetastatic niche (*50*). However, the link between the metabolic shift of cancer cells and P requirements may be more complex than we think. Recent evidence from murine models suggests that although cancer cells in primary

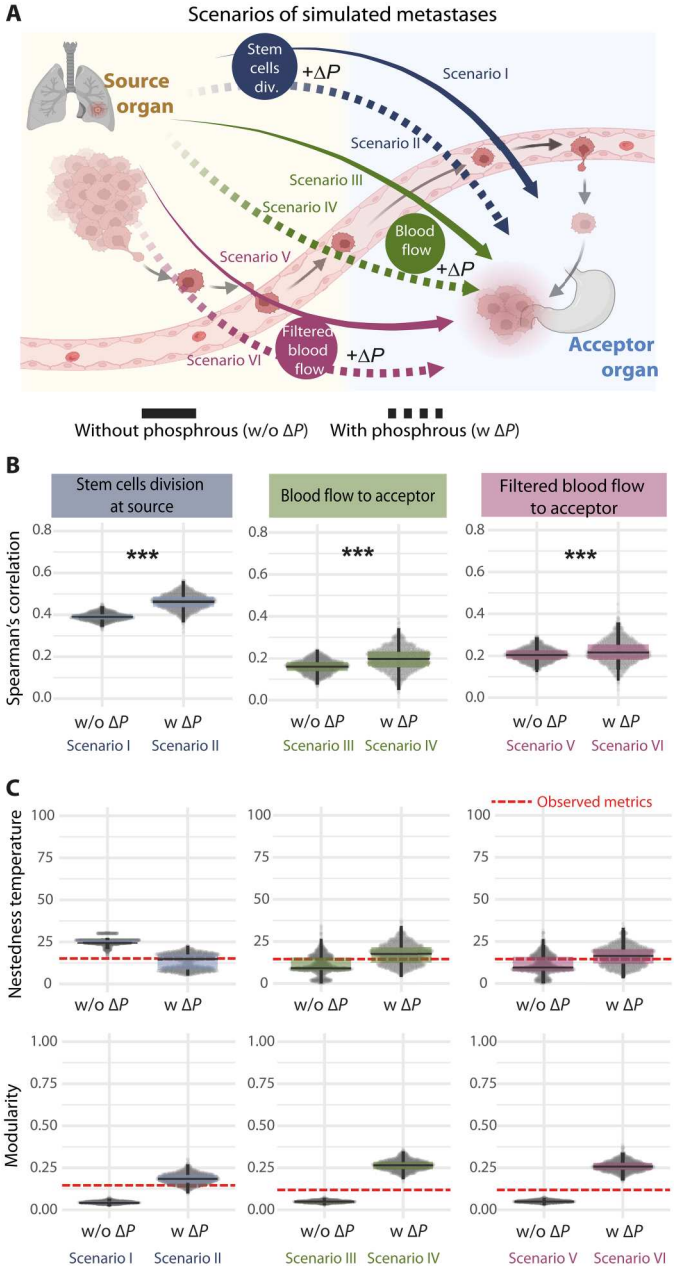

Fig. 3. Phosphorus gradients recapitulate macroscopic network properties. (**A**) Six scenarios to simulate the metastatic process with the probability of metastasis based on the organ's physiological attributes (cumulative lifetime stem cell divisions, blood flow, and phosphorus difference Δ*P*) and filtering of blood flow. (**B**) Spearman's correlation between observed and simulated metastatic relative occurrences where scenarios considering Δ*P* as a driver (w Δ*P*) have a significantly higher correlation with the observed metastatic relative occurrences compared to those without Δ*P* (w/o Δ*P*). ***$P < 0.001$, two-tailed *z* test. (**C**) Topological metrics of nestedness and modularity for the simulated networks. Thick horizontal lines in the boxplots indicate the median value of 5000 simulated networks (details in Materials and Methods). The first and third quartiles are represented by the box edges, and vertical lines indicate 1.5 times the interquartile range. The segmented horizontal red line in each plot corresponds to the indices calculated from the observed metastatic network in each case. (A) was made using BioRender (www.biorender.com).

orthotopic breast tumors showed the expected reduction in oxidative metabolism, this was increased in lung metastases (*51*). Further experimental studies exploring the energetic landscape across organs, under different health and neoplastic conditions, are required to further advance our understanding of the mechanisms underlying ATP production and its relation to P requirements in cancer cells.

A legacy effect, however, seems to be in action such that the priming of the stoichiometric niche of the pioneer migrant diaspora acquired in the source tissue affects its future success of invading a secondary organ (*16*), such as has been suggested for lung cancer (*17*) and shown for metastatic breast cancer (*39*, *40*). This is analogous to a maternal effect, as known in evolutionary ecology, whereby there is a causal influence of the maternal genotype or phenotype (i.e., the primary organ) on the offspring phenotype (i.e., the primary tumor and its metastatic propagules). In the case of cancer, since the original healthy cell already grows under a given phosphorus availability, that basal nutrient requirement is passed on, as a constraint, to the tumor cells and their metastases.

Phosphorus dynamics have been associated with overall cancer risk in the Swedish population (*52*), in lung cancer (*53*, *54*), and with an increased risk of lethal and high-grade prostate cancer (*55*, *56*). Consequently, phosphorus could be a marker for tumor progression (*22*, *57*, *58*), and the expression of phosphorus-associated genes, e.g., *ABCC11*, could serve as biomarkers of metastasis. Phosphates are also involved in protein phosphorylation (*59*) and act as a mitogenic factor inducing proliferation and activating cellular growth (*60*). Inorganic phosphate may promote the establishment of cancer cells via cell-mediated angiogenesis, dependent on the forkhead box protein C2, osteopontin, and vascular endothelial growth factor α (*61*). Moreover, the vitamin D–dependent regulation of cell morphology could be associated with phosphorus metabolism (*62*, *63*) and coupled with the effect of chemokines, such as CXCL8, regulating the epithelial-mesenchymal transition (EMT) and immune infiltration (*64*). Although the mechanistic pathway between phosphorus and EMT is still unknown, the ecological stoichiometry of P may contribute to an integrative framework for unveiling epigenetic mechanisms underpinning EMT (*65*, *66*) and the discovery of novel biomarkers and therapeutic targets.

Nutrient availability may affect not only growth dynamics at metastatic sites but also the migration process (*31*). Cell migration and invasion are the energy-intensive processes, requiring changes in cytoskeleton organization, synthesis of metalloproteinases, and microtubular remodeling during migration across the extracellular matrix from the primary tumor microenvironment and in the acceptor organ (*67*–*70*). These increased energetic costs are reflected in a positive correlation between migration potential and intracellular ATP:adenosine 5′-diphosphate ratio (*68*) and the selection of migration paths that require less energy (*71*). Thus, it is expected that migrating cells will follow resource gradients (*70*). In this context, our data suggest that cell migration could, in particular, be affected by gradients in key resources for ATP synthesis and growth, such as phosphorus. Nevertheless, our data are limited, and further tests of our predictions together with a comprehensive understanding and prediction of metastatic routes will come once we are able to produce systematic data on the human body ecosystem, from cells, as well as organs, to epidemiological and macroecological patterns.

Ecological insights have proven helpful in the study of cancer dynamics (*72*, *73*). A network approach coupled with an ecological framework provides new insights into metastatic phenomena (*74*) by studying macroscopic attributes (nestedness, degree distribution, and modularity), which are common in other complex systems (*75*–*77*). Harnessing niche and stoichiometric ecological theories (*19*, *29*, *32*) show that the emerging macroscopic patterns of metastatic incidence result from local ecologies orchestrating the habitat suitability for metastatic spread. Thus, ecological analysis of individuals as ecosystems could be essential to understanding tumor biology, evolution, and clinical progression, providing a framework for potential therapeutic targets.

MATERIALS AND METHODS

All statistical analyses were made in R (version 4.1.0) using the indicated packages. A comprehensive and interactive coding guide for the full reproducibility of this work is available at https://simonpcastillo.github.io/metastaticdiaspora. Source files are publicly available at Zenodo (https://doi.org/10.5281/zenodo.8408295).

Metastatic records

We studied the metastatic network by constructing a bipartite network between organs as nodes where a primary neoplasm in a source organ generated metastasis in an acceptor organ. In operational terms, the metastatic link is quantified as the number of metastases from a source to an acceptor organ. We included 9303 metastatic occurrences from five different sources (*78*–*82*). These medical records are from the United States, Switzerland, Germany, and Slovenia, taken between 1885 and 2009 (view references for years and occurrences). On the basis of Disibio and French (*78*), 33 anatomical zones (hereafter, "organs") were initially recorded, maintaining most of the organs present in (*78*). Given the constraints of the data, we were unable to filter by sex or other demographic categories, but we decided to exclude organs commonly associated with sex (breast, prostate, penis, testicles, uterus, vulva, vagina, and ovaries). In addition, we grouped organs as follows to reconcile contrasting terminology between studies: large intestine (colon, rectum, and anus), small intestine (appendix, duodenum, and small intestines), and head and neck (neck, lip, pharynx, salivary glands, and tonsil). After this data filtering, a total of 28 organs and 9303 occurrences were included in the analysis on the basis of autopsies and tomographies in the case of muscular cancers.

Network analysis

We define the metastatic process as a graph $G = (S, A, E)$, where S and A denote the set of source and acceptor organs, respectively, and E identifies the links connecting them, which, in this case, represents occurrences. We studied the weighted network $W = G = (S, A, E)$ of source-acceptor organ interactions $S \times A$ with $S = A = \{s_i, a_j, ..., N\}$, with $i, j \in N$ and N corresponds to the 28 organs. The network is studied as a matrix where each entry represents the metastatic process quantified by $n_{i,j}$ corresponding to the number of occurrences of the metastatic pair source-acceptor, i.e., the number of reported secondary growth metastases in an acceptor organ i that originated from a primary tumor in a source organ j. For network calculations, each cell value $n_{i,j}$ was transformed to a metastatic

relative occurrence value, calculated as $w_{i,j} = n_{i,j}/T$, with T being the total number of cases (9303 cases).

We quantify three main macroscopic attributes of the metastatic incidence network: nestedness (*76*, *83*), the distribution of metastatic links (degree distribution) (*84*), and modularity (*85*). All indices to estimate these attributes are available in the R package bipartite (*86*). We quantify nestedness using the nestedness temperature, NODF2, and the WINE (*87*). For the degree distribution, we used a modified version of the bipartite::degreedistr() function to find the best fit among exponential, power-law, and truncated power-law distributions based on R^2, Akaike's information criterion, and the Bayesian information criterion. For modularity, we compute modularity and module detection based on the Beckett algorithm as suggested for the case of weighted bipartite networks (*85*) method available in bipartite.

To discard spurious macroscopic attributes resulting from sampling effects, we compared the observed estimates against two types of null models with 1000 replicates each [package vegan (*88*)]. The first and second null models, in addition to maintaining the total number of occurrences, keep the marginal sum of source (method "r0_ind") and acceptor organ (method "c0_ind") occurrences, respectively. In fig. S1, we present the raw values of nestedness and modularity and the corresponding z-score for each model. To compare the observed network metrics (nestedness, degree distribution, and modularity) with null models, we performed a z test between the observed raw estimators against the estimators calculated from the null networks.

Vascular, physiological, and stoichiometric data

As an approach to evaluating Ewing's structural hypothesis, we assembled a binary vascular matrix representing spatial relationship between organs where an occurrence denotes the existence of a shared main blood vessel, hence both organs coexisting in a vascular territory. For example, the adrenal glands share blood supply with the esophagus and the diaphragm through the inferior phrenic arteries. We tested the statistical association between the resulting vascular matrix and the metastatic incidence matrix using Kendall's rank correlation.

Physiological data were only available for 21 of the 28 organs (table S2). We evaluate the hypothesis that cancer metastatic incidence of primary tumors in source organs and the source organ degree are associated with the cumulative number of stem cell divisions in a lifetime. In the case of acceptor organs, we evaluated whether the blood flux (in milliliters per minute per gram) could have a significant effect on the success of neoplastic propagules invading acceptor tissue, i.e., explaining acceptor metastatic incidence and the acceptor organ degree.

To assess the seed and soil hypothesis and unveil the effect of stoichiometry (organ nutrient composition) on metastatic incidence, we obtained literature-based estimates of macronutrient content (in grams) for a subset of organs adjusted by organ size, hereafter organ's mass-adjusted P content, abbreviated as P.g (grams of P over grams organ's mass; $n = 19$; table S3). Hence, we built an $n \times n$ subnetwork with the source-acceptor difference in the nutrients in each entry ($\Delta P = \text{P.g}^{\text{source}} - \text{P.g}^{\text{acceptor}}$). To quantitatively assess the pattern, we performed binomial regressions between the source or acceptor organ's degree as a function of the organ's mass-adjusted P content. In addition, we evaluated the effect of ΔP on occurrences and absences of metastases using a zero-inflated regression model with a Poisson distribution (log link) for occurrences and a binomial distribution (logit link) for absences, package pscl (*89*). For visualization, we computed nonlinear quantile regression for the first, fifth, and ninth deciles.

Incidence of primary tumors data

To evaluate the association between phosphorus content and the incidence of primary tumors, we matched the organ's P.g records with age-adjusted cancer incidence for $N = 11$ organs obtained from the Surveillance, Epidemiology, and End Results Program for the years 1999 to 2003, including males and females (*42*). After logarithmic transformation on both variables, we used Pearson's correlation to test the strength of the association.

Simulated metastases and emerging properties

To evaluate whether the observed physiological and stoichiometric relationships could reproduce the observed network structure in terms of nestedness and modularity, we simulate four different metastatic scenarios (see below), with 1000 replicates for each scenario. The number of organs in each scenario corresponds to the data availability (table S3). For each simulated metastatic network, we run 10,000 random metastatic events. A metastatic link is defined by the probability of metastasis $P_{j,i}$ from a source organ $i \in S$ to an acceptor organ $j \in A$ depending on the following:

Scenario I: The lifetime cumulative number of stem cell divisions in the source organ i (cumlscd_i)

$$Pr_{j,i} = \frac{\text{cumlscd}_i}{\sum_{i=1}^{S} \text{cumlscd}_i}$$

Scenario II: Scenario I multiplied by the normalized difference in phosphorus content between the corresponding source and acceptor pair

$$Pr_{j,i} = \frac{\text{cumlscd}_i}{\sum_{i=1}^{S} \text{cumlscd}_i} \times \frac{\Delta \text{P}_{j,i}}{\sum_{i=1}^{A} \Delta \text{P}_{j,i}}$$

Scenario III: The blood flow (flow) to an acceptor organ j

$$Pr_{j,i} = \frac{\text{flow}_j}{\sum_{j=1}^{A} \text{flow}_j}$$

Scenario IV: Scenario III multiplied by the difference in normalized phosphorus content between the corresponding source and acceptor pair

$$Pr_{j,i} = \frac{\text{flow}_j}{\sum_{j=1}^{A} \text{flow}_j} \times \frac{\Delta \text{P}_{j,i}}{\sum_{i=1}^{A} \Delta \text{P}_{j,i}}$$

To account for blood filtering in the liver coming from GI organs, two other scenarios consider that when by chance a GI primary tumor and nonliver organs are chosen during the simulation, the probability of metastasis $Pr_{j,i}$ is halved [filter flow sensu (*13*)]. Then, scenarios V and VI are the same as scenarios III and

IV, respectively, except for primary gastric tumors which $P_{j,i}$ is halved because of a filtering of blood in the liver.

Since P can take negative values, we transformed it by adding the absolute value of min(ΔP). The ratio $\frac{\Delta P_{j,i}}{\sum_{i=1}^{A} \Delta P_{j,i}}$ was then calculated across acceptor organs for each source. We did not simulate a network scenario with all three factors (lscdcum, flow, and ΔP) included because of only five organs with records for all these parameters.

For each simulated network, metastatic relative occurrences were calculated as the number of successful metastatic links for a source-acceptor pair over the total number of links. In addition, topological descriptors of nestedness (temperature, NODF, and WINE) and modularity were calculated for each simulated network. We compared these metrics from the simulated metastases with the observed topological descriptors recalculated on the basis of the organs considered in the simulation. We computed Pearson's correlation between the two matrices to compare the observed and simulated metastatic incidence matrix for each case. Last, we compared the observed nestedness and modularity indices with values calculated for the simulated networks between scenarios for which we obtained mean/median values and the range.

Supplementary Materials

This PDF file includes:

Fig. S1 to S4
Tables S1 to S4
References

REFERENCES AND NOTES

1. H. Dillekås, M. S. Rogers, O. Straume, Are 90% of deaths from cancer caused by metastases? *Cancer Med.* **8**, 5574–5576 (2019).
2. D. Hanahan, R. A. Weinberg, The hallmarks of cancer. *Cell* **100**, 57–70 (2000).
3. Y. Gao, I. Bado, H. Wang, W. Zhang, J. M. Rosen, X. H.-F. Zhang, Metastasis organotropism: Redefining the congenial soil. *Dev. Cell* **49**, 375–391 (2019).
4. S. Paget, The distribution of secondary growths in cancer of the breast. *The Lancet.* **133**, 571–573 (1889).
5. A. E. de Groot, S. Roy, J. S. Brown, K. J. Pienta, S. R. Amend, Revisiting seed and soil: Examining the primary tumor and cancer cell foraging in metastasis. *Mol. Cancer Res.* **15**, 361–370 (2017).
6. J. Grinnell, Field tests of theories concerning distributional control. *Am. Nat.* **51**, 115–128 (1917).
7. J. Ewing, Neoplastic diseases, a treatise on tumors. *Can. Med. Assoc. J.* **14**, 466 (1924).
8. J. Massagué, K. Ganesh, Metastasis-initiating cells and ecosystems. *Cancer Discov.* **11**, 971–994 (2021).
9. C. Tomasetti, R. Durrett, M. Kimmel, A. Lambert, G. Parmigiani, A. Zauber, B. Vogelstein, Role of stem-cell divisions in cancer risk. *Nature* **548**, E13–E14 (2017).
10. J. Massagué, A. C. Obenauf, Metastatic colonization by circulating tumour cells. *Nature* **529**, 298–306 (2016).
11. I. J. Fidler, The organ microenvironment and cancer metastasis. *Differentiation* **70**, 498–505 (2002).
12. F. Font-Clos, S. Zapperi, C. A. M. La Porta, Blood flow contributions to cancer metastasis. *iScience* **23**, 101073 (2020).
13. J. G. Scott, A. G. Fletcher, P. K. Maini, A. R. A. Anderson, P. Gerlee, A filter-flow perspective of haematogenous metastasis offers a non-genetic paradigm for personalised cancer therapy. *Eur. J. Cancer* **50**, 3068–3075 (2014).
14. J. Scott, P. Kuhn, A. R. A. Anderson, Unifying metastasis — Integrating intravasation, circulation and end-organ colonization. *Nat. Rev. Cancer* **12**, 445–446 (2012).
15. A. S. Azevedo, G. Follain, S. Patthabhiraman, S. Harlepp, J. G. Goetz, Metastasis of circulating tumor cells: Favorable soil or suitable biomechanics, or both? *Cell Adh. Migr.* **9**, 345–356 (2015).
16. T. Schild, V. Low, J. Blenis, A. P. Gomes, Unique metabolic adaptations dictate distal organ-specific metastatic colonization. *Cancer Cell* **33**, 347–354 (2018).
17. C. Martínez-Ruiz, J. R. M. Black, C. Puttick, M. S. Hill, J. Demeulemeester, E. Larose Cadieux, K. Thol, T. P. Jones, S. Veeriah, C. Naceur-Lombardelli, A. Toncheva, P. Prymas, A. Rowan, S. Ward, L. Cubitt, F. Athanasopoulou, O. Pich, T. Karasaki, D. A. Moore, R. Salgado, E. Colliver, C. Castignani, M. Dietzen, A. Huebner, M. Al Bakir, M. Tanić, T. B. K. Watkins, E. L. Lim, A. M. Al-Rashed, D. Lang, J. Clements, D. E. Cook, R. Rosenthal, G. A. Wilson, A. M. Frankell, S. de Carné Trécesson, P. East, N. Kanu, K. Litchfield, N. J. Birkbak, A. Hackshaw, S. Beck, P. Van Loo, M. Jamal-Hanjani; TRACERx Consortium, C. Swanton, N. McGranahan, Genomic–transcriptomic evolution in lung cancer and metastasis. *Nature* **616**, 543–552 (2023).
18. M. Al Bakir, A. Huebner, C. Martínez-Ruiz, K. Grigoriadis, T. B. K. Watkins, O. Pich, D. A. Moore, S. Veeriah, S. Ward, J. Laycock, D. Johnson, A. Rowan, M. Razaq, M. Akther, C. Naceur-Lombardelli, P. Prymas, A. Toncheva, S. Hessey, M. Dietzen, E. Colliver, A. M. Frankell, A. Bunkum, E. L. Lim, T. Karasaki, C. Abbosh, C. T. Hiley, M. S. Hill, D. E. Cook, G. A. Wilson, R. Salgado, E. Nye, R. K. Stone, D. A. Fennell, G. Price, K. M. Kerr, B. Naidu, G. Middleton, Y. Summers, C. R. Lindsay, F. H. Blackhall, J. Cave, K. G. Blyth, A. Nair, A. Ahmed, M. N. Taylor, A. J. Procter, M. Falzon, D. Lawrence, N. Navani, R. M. Thakrar, S. M. Janes, D. Papadatos-Pastos, M. D. Forster, S. M. Lee, T. Ahmad, S. A. Quezada, K. S. Peggs, P. Van Loo, C. Dive, A. Hackshaw, N. J. Birkbak, S. Zaccaria; TRACERx Consortium, M. Jamal-Hanjani, N. McGranahan, C. Swanton, The evolution of non-small cell lung cancer metastases in TRACERx. *Nature* **616**, 534–542 (2023).
19. J. J. Elser, M. M. Kyle, M. S. Smith, J. D. Nagy, Biological stoichiometry in human cancer. *PLOS ONE* **2**, e1028 (2007).
20. C. C. C. R. de Carvalho, M. J. Caramujo, Tumour metastasis as an adaptation of tumour cells to fulfil their phosphorus requirements. *Med. Hypotheses* **78**, 664–667 (2012).
21. N. Hernando, K. Gagnon, E. Lederer, Phosphate transport in epithelial and nonepithelial tissue. *Physiol. Rev.* **101**, 1–35 (2021).
22. M. A. Lacerda-Abreu, T. Russo-Abrahão, R. de Queiroz Monteiro, F. D. Rumjanek, J. R. Meyer-Fernandes, Inorganic phosphate transporters in cancer: Functions, molecular mechanisms and possible clinical applications. *Biochim. Biophys. Acta Rev. Cancer* **1870**, 291–298 (2018).
23. R. Y. Ebright, S. Lee, B. S. Wittner, K. L. Niederhoffer, B. T. Nicholson, A. Bardia, S. Truesdell, D. F. Wiley, B. Wesley, S. Li, A. Mai, N. Aceto, N. Vincent-Jordan, A. Szabolcs, B. Chirn, J. Kreuzer, V. Comaills, M. Kalinich, W. Haas, D. T. Ting, M. Toner, S. Vasudevan, D. A. Haber, S. Maheswaran, D. S. Micalizzi, Deregulation of ribosomal protein expression and translation promotes breast cancer metastasis. *Science* **367**, 1468–1473 (2020).
24. J. M. Dolezal, A. P. Dash, E. V. Prochownik, Diagnostic and prognostic implications of ribosomal protein transcript expression patterns in human cancers. *BMC Cancer* **18**, 275 (2018).
25. P. Vaupel, H. Schmidberger, A. Mayer, The Warburg effect: Essential part of metabolic reprogramming and central contributor to cancer progression. *Int. J. Radiat. Biol.* **95**, 912–919 (2019).
26. T. Pfeiffer, S. Schuster, S. Bonhoeffer, Cooperation and competition in the evolution of ATP-producing pathways. *Science* **292**, 504–507 (2001).
27. J. Chen, K. Sprouffske, Q. Huang, C. C. Maley, Solving the puzzle of metastasis: The evolution of cell migration in neoplasms. *PLOS ONE* **6**, e17933 (2011).
28. W. Lu, Y. Hu, G. Chen, Z. Chen, H. Zhang, F. Wang, L. Feng, H. Pelicano, H. Wang, M. J. Keating, J. Liu, W. McKeehan, H. Wang, Y. Luo, P. Huang, Novel role of NOX in supporting aerobic glycolysis in cancer cells with mitochondrial dysfunction and as a potential target for cancer therapy. *PLoS Biol.* **10**, e1001326 (2012).
29. K. Kim, H. Huang, P. K. Parida, L. He, M. Marquez-Palencia, T. C. Reese, P. Kapur, J. Brugarolas, R. A. Brekken, S. Malladi, Cell competition shapes metastatic latency and relapse. *Cancer Discov.* **13**, 85–97 (2023).
30. G. Bergers, S.-M. Fendt, The metabolism of cancer cells during metastasis. *Nat. Rev. Cancer* **21**, 162–180 (2021).
31. I. J. Bettum, S. S. Gorad, A. Barkovskaya, S. Pettersen, S. A. Moestue, K. Vasiliauskaite, E. Tenstad, T. Øyjord, Ø. Risa, V. Nygaard, G. M. Mælandsmo, L. Prasmickaite, Metabolic reprogramming supports the invasive phenotype in malignant melanoma. *Cancer Lett.* **366**, 71–83 (2015).
32. A. L. González, O. Dézerald, P. A. Marquet, G. Q. Romero, D. S. Srivastava, The multidimensional stoichiometric niche. *Front. Ecol. Evol.* 5 10.3389/fevo.2017.00110, (2017).
33. J. E. Keymer, P. A. Marquet, The complexity of cancer ecosystems, in *Frontiers in Ecology, Evolution and Complexity*, M. Benitez, O. Miramontes, A. Valiente-Banuet, Eds. (CopltarXives, 2014), p. 21.
34. M. S. Mariani, Z.-M. Ren, J. Bascompte, C. J. Tessone, Nestedness in complex networks: Observation, emergence, and implications. *Phys. Rep.* **813**, 1–90 (2019).

35. B. D. Patterson, On the temporal development of nested subset patterns of species composition. *Oikos* **59**, 330–342 (1990).
36. P. Jordano, J. Bascompte, J. M. Olesen, Invariant properties in coevolutionary networks of plant–animal interactions. *Ecol. Lett.* **6**, 69–81 (2003).
37. D. M. Richardson, P. Pyšek, Plant invasions: Merging the concepts of species invasiveness and community invasibility. *Prog. Phys. Geogr.* **30**, 409–431 (2006).
38. J. E. Keymer, P. A. Marquet, J. X. Velasco-Hernández, S. A. Levin, A. E. L. Fahrig, Extinction thresholds and metapopulation persistence in dynamic landscapes. *Am. Nat.* **156**, 478–494 (2000).
39. M. Fiorillo, B. Ózsvári, F. Sotgia, M. P. Lisanti, High ATP production fuels cancer drug resistance and metastasis: Implications for mitochondrial ATP depletion therapy. *Front. Oncol.* **11**, 740720 (2021).
40. M. B. Jekabsons, M. Merrell, A. G. Skubiz, N. Thornton, S. Milasta, D. Green, T. Chen, Y.-H. Wang, B. Avula, I. A. Khan, Y.-D. Zhou, Breast cancer cells that preferentially metastasize to lung or bone are more glycolytic, synthesize serine at greater rates, and consume less ATP and NADPH than parent MDA-MB-231 cells. *Cancer Metab.* **11**, 4 (2023).
41. "Report of the task group on reference man," *ICRP Publication* (no. 23), (Pergamon Press, 1975.
42. M. J. Hayat, N. Howlader, M. E. Reichman, B. K. Edwards, Cancer statistics, trends, and multiple primary cancer analyses from the surveillance, epidemiology, and end results (SEER) program. *Oncologist* **12**, 20–37 (2007).
43. C. Tomasetti, B. Vogelstein, Variation in cancer risk among tissues can be explained by the number of stem cell divisions. *Science* **347**, 78–81 (2015).
44. S. R. Amend, K. J. Pienta, Ecology meets cancer biology: The cancer swamp promotes the lethal cancer phenotype. *Oncotarget* **6**, 9669–9678 (2015).
45. S. R. Amend, R. A. Gatenby, K. J. Pienta, J. S. Brown, Cancer foraging ecology: Diet choice, patch use, and habitat selection of cancer cells. *Curr. Pathobiol. Rep.* **6**, 209–218 (2018).
46. R. R. Langley, I. J. Fidler, The seed and soil hypothesis revisited—The role of tumor-stroma interactions in metastasis to different organs. *Int. J. Cancer* **128**, 2527–2535 (2011).
47. A. L. González, J. S. Kominoski, M. Danger, S. Ishida, N. Iwai, A. Rubach, Can ecological stoichiometry help explain patterns of biological invasions? *Oikos* **119**, 779–790 (2010).
48. S. Jones, W.-D. Chen, G. Parmigiani, F. Diehl, N. Beerenwinkel, T. Antal, A. Traulsen, M. A. Nowak, C. Siegel, V. E. Velculescu, K. W. Kinzler, B. Vogelstein, J. Willis, S. D. Markowitz, Comparative lesion sequencing provides insights into tumor evolution. *Proc. Natl. Acad. Sci. U.S.A.* **105**, 4283–4288 (2008).
49. S. Yachida, S. Jones, I. Bozic, T. Antal, R. Leary, B. Fu, M. Kamiyama, R. H. Hruban, J. R. Eshleman, M. A. Nowak, V. E. Velculescu, K. W. Kinzler, B. Vogelstein, C. A. Iacobuzio-Donahue, Distant metastasis occurs late during the genetic evolution of pancreatic cancer. *Nature* **467**, 1114–1117 (2010).
50. G. Doglioni, S. Parik, S.-M. Fendt, Interactions in the (pre)metastatic niche support metastasis formation. *Oncology* **9**, 219 (2019).
51. C. R. Bartman, D. R. Weilandt, Y. Shen, W. D. Lee, Y. Han, T. TeSlaa, C. S. R. Jankowski, L. Samarah, N. R. Park, V. da Silva-Diz, M. Aleksandrova, Y. Gultekin, A. Marishta, L. Wang, L. Yang, A. Roichman, V. Bhatt, T. Lan, Z. Hu, X. Xing, W. Lu, S. Davidson, M. Wühr, M. G. Vander Heiden, D. Herranz, J. Y. Guo, Y. Kang, J. D. Rabinowitz, Slow TCA flux and ATP production in primary solid tumours but not metastases. *Nature* **614**, 349–357 (2023).
52. W. Wulaningsih, K. Michaelsson, H. Garmo, N. Hammar, I. Jungner, G. Walldius, L. Holmberg, M. Van Hemelrijck, Inorganic phosphate and the risk of cancer in the Swedish AMORIS study. *BMC Cancer* **13**, 257 (2013).
53. H. Jin, C.-X. Xu, H.-T. Lim, S.-J. Park, J.-Y. Shin, Y.-S. Chung, S.-C. Park, S.-H. Chang, H.-J. Youn, K.-H. Lee, Y.-S. Lee, Y.-C. Ha, C.-H. Chae, G. R. Beck, M.-H. Cho, High dietary inorganic phosphate increases lung tumorigenesis and alters Akt signaling. *Am. J. Respir. Crit. Care Med.* **179**, 59–68 (2009).
54. C. Friedrich, S. Schallenberg, M. Kirchner, M. Ziehm, S. Niquet, M. Haji, C. Beier, J. Neudecker, F. Klauschen, P. Mertins, Comprehensive micro-scaled proteome and phosphoproteome characterization of archived retrospective cancer repositories. *Nat. Commun.* **12**, 3576 (2021).
55. K. M. Wilson, I. M. Shui, L. A. Mucci, E. Giovannucci, Calcium and phosphorus intake and prostate cancer risk: A 24-y follow-up study. *Am. J. Clin. Nutr.* **101**, 173–183 (2015).
56. J. M. Drake, E. O. Paull, N. A. Graham, J. K. Lee, B. A. Smith, B. Titz, T. Stoyanova, C. M. Faltermeier, V. Uzunangelov, D. E. Carlin, D. T. Fleming, C. K. Wong, Y. Newton, S. Sudha, A. A. Vashisht, J. Huang, J. A. Wohlschlegel, T. G. Graeber, O. N. Witte, J. M. Stuart, Phosphoproteome integration reveals patient-specific networks in prostate cancer. *Cell* **166**, 1041–1054 (2016).
57. A. A. Bobko, T. D. Eubank, B. Driesschaert, I. Dhimitruka, J. Evans, R. Mohammad, E. E. Tchekneva, M. M. Dikov, V. V. Khramtsov, Interstitial inorganic phosphate as a tumor microenvironment marker for tumor progression. *Sci. Rep.* **7**, 41233 (2017).
58. S. Venturelli, C. Leischner, T. Helling, O. Renner, M. Burkard, L. Marongiu, Minerals and cancer: Overview of the possible diagnostic value. *Cancer* **14**, 1256 (2022).
59. H. C. Harsha, A. Pandey, Phosphoproteomics in cancer. *Mol. Oncol.* **4**, 482–495 (2010).
60. R. B. Brown, M. S. Razzaque, Phosphate toxicity and tumorigenesis. *Biochim. Biophys. Acta Rev. Cancer* **1869**, 303–309 (2018).
61. Y. Lin, K. E. McKinnon, S. W. Ha, G. R. Beck, Inorganic phosphate induces cancer cell mediated angiogenesis dependent on forkhead box protein C2 (FOXC2) regulated osteopontin expression. *Mol. Carcinog.* **54**, 926–934 (2015).
62. G. Jacquillet, R. J. Unwin, Physiological regulation of phosphate by vitamin D, parathyroid hormone (PTH) and phosphate (Pi). *Pflugers Arch.* **471**, 83–98 (2019).
63. A. Fernández-Barral, P. Bustamante-Madrid, G. Ferrer-Mayorga, A. Barbáchano, M. J. Larriba, A. Muñoz, Vitamin D effects on cell differentiation and stemness in cancer. *Cancer* **12**, 2413 (2020).
64. S. Singh, A. P. Singh, B. Sharma, L. B. Owen, R. K. Singh, CXCL8 and its cognate receptors in melanoma progression and metastasis. *Future Oncol.* **6**, 111–116 (2010).
65. Y.-T. Lin, K.-J. Wu, Epigenetic regulation of epithelial-mesenchymal transition: Focusing on hypoxia and TGF-β signaling. *J. Biomed. Sci.* **27**, 39 (2020).
66. R. C. J. D'Souza, A. M. Knittle, N. Nagaraj, M. van Dinther, C. Choudhary, P. ten Dijke, M. Mann, K. Sharma, Time-resolved dissection of early phosphoproteome and ensuing proteome changes in response to TGF-β. *Sci. Signal.* **7**, rs5 (2014).
67. L. A. Liotta, W. G. Stetler-Stevenson, Metalloproteinases and cancer invasion. *Semin. Cancer Biol.* **1**, 99–106 (1990).
68. M. R. Zanotelli, Z. E. Goldblatt, J. P. Miller, F. Bordeleau, J. Li, J. A. VanderBurgh, M. C. Lampi, M. R. King, C. A. Reinhart-King, Regulation of ATP utilization during metastatic cell migration by collagen architecture. *Mol. Biol. Cell* **29**, 1–9 (2018).
69. M. R. Zanotelli, J. Zhang, C. A. Reinhart-King, Mechanoresponsive metabolism in cancer cell migration and metastasis. *Cell Metab.* **33**, 1307–1321 (2021).
70. L. Liu, G. Duclos, B. Sun, J. Lee, A. Wu, Y. Kam, E. D. Sontag, H. A. Stone, J. C. Sturm, R. A. Gatenby, R. H. Austin, Minimization of thermodynamic costs in cancer cell invasion. *Proc. Natl. Acad. Sci.* **110**, 1686–1691 (2013).
71. M. R. Zanotelli, A. Rahman-Zaman, J. A. VanderBurgh, P. V. Taufalele, A. Jain, D. Erickson, F. Bordeleau, C. A. Reinhart-King, Energetic costs regulated by cell mechanics and confinement are predictive of migration path during decision-making. *Nat. Commun.* **10**, 4185 (2019).
72. M. E. Hochberg, R. J. Noble, A framework for how environment contributes to cancer risk. *Ecol. Lett.* **20**, 117–134 (2017).
73. C. C. Maley, A. Aktipis, T. A. Graham, A. Sottoriva, A. M. Boddy, M. Janiszewska, A. S. Silva, M. Gerlinger, Y. Yuan, K. J. Pienta, K. S. Anderson, R. Gatenby, C. Swanton, D. Posada, C.-I. Wu, J. D. Schiffman, E. S. Hwang, K. Polyak, A. R. A. Anderson, J. S. Brown, M. Greaves, D. Shibata, Classifying the evolutionary and ecological features of neoplasms. *Nat. Rev. Cancer* **17**, 605–619 (2017).
74. L. L. Chen, N. Blumm, N. A. Christakis, A.-L. Barabási, T. S. Deisboeck, Cancer metastasis networks and the prediction of progression patterns. *Br. J. Cancer* **101**, 749–758 (2009).
75. A.-L. Barabási, Scale-free networks: A decade and beyond. *Science* **325**, 412–413 (2009).
76. M. Cantor, M. M. Pires, F. M. D. Marquitti, R. L. G. Raimundo, E. Sebastián-González, P. P. Coltri, S. I. Perez, D. R. Barneche, D. Y. C. Brandt, K. Nunes, F. G. Daura-Jorge, S. R. Floeter, P. R. Guimarães Jr., Nestedness across biological scales. *PLOS ONE* **12**, e0171691 (2017).
77. M. A. Fortuna, D. B. Stouffer, J. M. Olesen, P. Jordano, D. Mouillot, B. R. Krasnov, R. Poulin, J. Bascompte, Nestedness versus modularity in ecological networks: Two sides of the same coin? *J. Anim. Ecol.* **79**, 811–817 (2010).
78. G. Disibio, S. W. French, Metastatic patterns of cancers: Results from a large autopsy study. *Arch. Pathol. Lab. Med.* **132**, 931–939 (2008).
79. J. K. Patel, M. S. Didolkar, J. W. Pickren, R. H. Moore, Metastatic pattern of malignant melanoma. *Am. J. Surg.* **135**, 807–810 (1978).
80. H. L. Abrams, R. Spiro, N. Goldstein, Metastases in carcinoma. Analysis of 1000 autopsied cases. *Cancer* **3**, 74–85 (1950).
81. A. B. Shinagare, N. H. Ramaiya, J. P. Jagannathan, F. M. Fennessy, M.-E. Taplin, A. D. Van den Abbeele, Metastatic pattern of bladder cancer: Correlation with the characteristics of the primary tumor. *Am. J. Roentgenol.* **196**, 117–122 (2011).
82. E. S. Nussbaum, H. R. Djalilian, K. H. Cho, W. A. Hall, Brain metastases: Histology, multiplicity, surgery, and survival. *Cancer* **78**, 1781–1788 (1996).
83. B. D. Patterson, W. Atmar, Nested subsets and the structure of insular mammalian faunas and archipelagos. *Biol. J. Linn. Soc.* **28**, 65–82 (1986).
84. A. Clauset, C. R. Shalizi, M. E. J. Newman, Power-law distributions in empirical data. *SIAM Rev.* **51**, 661–703 (2009).
85. S. J. Beckett, Improved community detection in weighted bipartite networks. *R. Soc. Open Sci.* **3**, 140536 (2016).
86. C. Dormann, B. Gruber, J. Fründ, Introducing the bipartite package: Analysing ecological networks. *R News.* **8**, 8–11 (2008).

87. J. Galeano, J. M. Pastor, J. M. Iriondo, Weighted-interaction nestedness estimator (WINE): A new estimator to calculate over frequency matrices. *Environ. Model. Software* **24**, 1342–1346 (2009).
88. J. Oksanen, F. G. Blanchet, R. Kindt, P. Legendre, P. R. Minchin, R. O'hara, G. L. Simpson, P. Solymos, M. H. H. Stevens, H. Wagner, Vegan: Community Ecology Package, version. 2, (2013) p. 1–295; https://cran.r-project.org/web/packages/vegan/index.html.
89. A. Zeileis, C. Kleiber, S. Jackman, Regression models for count data in R. *J. Stat. Softw.* **27**, 1–25 (2008).
90. J. Valentin, Basic anatomical and physiological data for use in radiological protection: Reference values: ICRP Publication 89. *Ann. ICRP* **32**, 1–277 (2002).

Acknowledgments: Several people provided discussion, pointed out dataset sets and provided statistical advice. Among them, we thank C. Maley, D. Gordon, J. Tylianakis, N. Roth, E. Tomas-Bort, and M. Yilales. We thank the constructive criticism made by the reviewers. The corresponding authors thank the space provided by The Santa Fe Institute to complete this work. **Funding:** This work was supported by National Agency of Research and Development of Chile ANID-Chile, grant PFCHA/DocNac/21170089 (to S.P.C.); the Fondation ARC pour la recherche sur le cancer: programmes labellisés 2021, grant ARCPGA12021010002850_3574 (to M.E.H.); National Agency of Research and Development of Chile ANID-Chile, Fondo de Desarrollo Científico y Tecnológico (FONDECYT), "The emergence of ecologies through metabolic cooperation and recursive organization," grants AFB 17008 and ANID-1200925 (to P. A.M.); National Agency of Research and Development of Chile ANID-Chile, BASAL funds for centers of excellence from ANID-Chile, Centro de Modelamiento Matemático (CMM), grants ACE210010 and FB210005 (to P.A.M.); National Agency of Research and Development of Chile ANID-Chile Centres of Excellence, grant ACE210010 (to P.A.M.). **Author contributions:** Conceptualization: S.P.C., P.A.M., and ME.H. Methodology: S.P.C., P.A.M., and R.A.R. Analyses: S.P. C., P.A.M., M.A., M.E.H., and R.A.R. Visualization: S.P.C. Biomedical advice: R.A.R. Writing—initial draft: S.P.C. and P.A.M. Writing—final draft: All authors. **Competing interests:** The authors declare that they have no competing interests. **Data and materials availability:** All data needed to evaluate the conclusions in the paper are present in the paper and/or the Supplementary Materials. Source files and codes are publicly available at Zenodo (https://doi.org/10.5281/zenodo.8408295). A comprehensive and interactive coding guide for the complete reproducibility of this work is available https://simonpcastillo.github.io/metastaticdiaspora.

Submitted 17 May 2023
Accepted 10 November 2023
Published 13 December 2023
10.1126/sciadv.adi7902